Impact of engineered surface microtopography on biofilm formation of *Staphylococcus aureus*

Kenneth K. Chung
Department of Materials Science and Engineering, University of Florida, Gainesville, Florida 32611

James F. Schumacher
J. Crayton Pruitt Family Department of Biomedical Engineering, University of Florida, Gainesville, Florida 32611

Edith M. Sampson
Department of Otolaryngology, University of Florida, Gainesville, Florida 32611

Robert A. Burne
Department of Oral Biology, UF College of Dentistry, University of Florida, Gainesville, Florida 32611

Patrick J. Antonelli
Department of Otolaryngology, University of Florida, Gainesville, Florida 32611

Anthony B. Brennan[a)]
Department of Materials Science and Engineering, and J. Crayton Pruitt Family Department of Biomedical Engineering, University of Florida, Gainesville, Florida 32611

(Received 29 March 2007; accepted 30 May 2007; published 29 June 2007)

The surface of an indwelling medical device can be colonized by human pathogens that can form biofilms and cause infections. In most cases, these biofilms are resistant to antimicrobial therapy and eventually necessitate removal or replacement of the device. An engineered surface microtopography based on the skin of sharks, Sharklet AF™, has been designed on a poly(dimethyl siloxane) elastomer (PDMSe) to disrupt the formation of bacterial biofilms without the use of bactericidal agents. The Sharklet AF™ PDMSe was tested against smooth PDMSe for biofilm formation of *Staphylococcus aureus* over the course of 21 days. The smooth surface exhibited early-stage biofilm colonies at 7 days and mature biofilms at 14 days, while the topographical surface did not show evidence of early biofilm colonization until day 21. At 14 days, the mean value of percent area coverage of *S. aureus* on the smooth surface was 54% compared to 7% for the Sharklet AF™ surface ($p < 0.01$). These results suggest that surface modification of indwelling medical devices and exposed sterile surfaces with the Sharklet AF™ engineered topography may be an effective solution in disrupting biofilm formation of *S. aureus*. © *2007 American Vacuum Society.* [DOI: 10.1116/1.2751405]

I. INTRODUCTION

Bacterial biofilms are a major concern in the development of biomaterials, ultrafiltration systems, and underwater vessels. In the biomedical arena, bacterial colonization of surfaces compromises the effectiveness of implanted materials and ultimately can result in persistent infections.[1,2] Biomaterial surfaces for tissue constructs and implants are subject to a competition between microbial adhesion and tissue integration, where an ideal surface would prevent the former while promoting the latter.[3] However, the chemical, mechanical, and physical properties of tissue construct materials are inherently meant to enhance all forms of biogrowth, making it equally likely that such a surface would submit to bacterial colonization.

Microorganisms colonize biomedical implants by developing biofilms, structured communities of microbial cells embedded in an extracellular polymeric matrix that are adherent to the implant and/or the host tissues.[2,4] Biofilms render microorganisms resistant to host defenses and antibiotic therapy.[5,6] The clinical means of managing biofilms has been prevention.

Preventing biofilm-associated infections has traditionally been through use of prophylactic antibacterial agents, whether delivered systemically or released directly from the biomaterial.[7] Pharmacokinetics and toxicity of the antibacterial agents incorporated in biomaterials have limited the effectiveness of such therapies.[7–10] Antibiotics, antibodies, and phagocytes can clear planktonic cells released by the biofilm, but the sessile communities themselves are resistant to such agents.[11,12] Antibiotic therapy resulting in incomplete eradication of biofilm has been linked with the emergence of antibiotic-resistant bacteria, which may compromise the effectiveness of these agents for even non-biofilm-mediated infections.[13–16]

Another strategy for preventing the development of biofilms has been to alter the biomaterial surface properties. Surface modification techniques to tailor the surface energy via surface chemistry and surface topography have been developed to study the effects of changes in these surface prop-

a)Electronic mail: abrennan@mse.ufl.edu

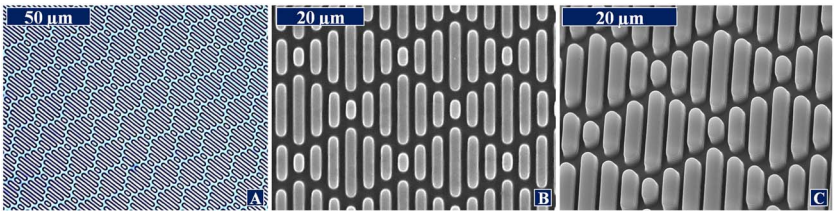

FIG. 1. Sharklet AF™ topography on poly(dimethyl siloxane) elastomer (PDMSe) with 2 μm feature width and spacing and 3 μm feature height. (A) Light micrograph with top-down view. (B) Scanning electron micrograph with top down view. (C) Scanning electron micrograph taken at 35° tilt to show protruding features.

erties on biofilm formation.[17,18] Bacterial adhesion has been investigated on surface topographies that range from random structures to ordered arrays. There appears to be a trend toward increased bacterial coverage as the R_a-roughness values increased on electropolished steel.[19] Conversely, *P. aeruginosa* was less likely to foul hydrophilic, electrically neutral, smooth polymeric surfaces.[20] Interestingly, bacterial adhesion was reduced on stainless steel surface microtopographies that were generated by a one-directional polishing finish relative to smooth surfaces.[21] The aforementioned studies examined surfaces that were randomly roughened and did not examine specific surface features. The effects of a nonrandom topography consisting of etched grooves of varying widths in silicon coupons with *P. aeruginosa* and *P. fluorescens* showed that rates of attachment were independent of groove size and greatest on the downstream edges of grooves.[22] More recently, microbial retention on a defined microtopography in the form of etched pits was determined to be dependent on both the size of the surface defect and the cell.[23]

The purpose of our study was to investigate the potential for bacterial attachment and colonization on an engineered topography with a well-defined structure. Our research is focused on the design and characterization of surface microtopographies that effectively control bioadhesion, with the goal to produce a biomaterial with topography variants that can effectively switch from biofilm forming to biofilm inhibition. To achieve this, a surface energy model was created correlating wettability with bioadhesion to characterize and develop settlement-enhancing as well as antifouling topographies.[24] The application of this model led to the design concept of a biomimetic structure inspired by the skin of fast-moving sharks (Sharklet AF™), and an engineered roughness index (ERI) was developed as an extension of this model to study and develop other unique engineered topographies.[25]

In this article, a surface of uniform chemistry with an engineered microtopography was investigated for the inhibition of bacterial biofilm formation. The most successful design to date is Sharklet AF™. This particular microtopography is unique from the aforementioned ones in that it has nonrandom, clearly defined surface features that are typically tailored to the critical dimensions of the fouling organism. Recent results on the Sharklet AF™ and other engineered microtopographies designed at a 2 μm feature width and spacing have shown a strong correlation between the ERI and the inhibition of settlement by the zoospores (~5 μm in diameter) of the most common ship fouling alga, *Ulva*.[25] In addition, the Sharklet AF™ microtopography designed at a 20 μm feature width and spacing has been demonstrated to be a strong inhibitor of the settlement of barnacle cyprids of *B. amphitrite*.[26] This organism's attachment disk measures ~25–30 μm.[27] For the present study, the *Ulva*-specific Sharklet AF™ surface was selected for the potential to inhibit biofilm formation of *Staphylococcus aureus* based on the approximate match between the size of the bacteria and the critical dimensions of this surface (2 μm feature width and spacing, 3 μm feature height). It was hypothesized that the dimensions of the topography would be slightly too large to effectively reduce the attachment of the bacteria in the size range of ~1–2 μm but could be effective at physically disrupting the further colonization of additional bacteria and subsequent formation of biofilm (Fig. 1). *S. aureus* was selected as the bacterial pathogen due to both its size and its association with nosocomial infections in implanted devices, such as cochlear implants, sutures, and heart valves.[10,28]

II. MATERIALS AND METHODS

A. Materials

Dow Corning® Silastic® T-2, a platinum-catalyzed poly(dimethyl siloxane) elastomer (PDMSe), was used for its low modulus, low surface energy, and propensity for minimal bioadhesion.[29] Silastic® brand silicone elastomers are biomaterials used in numerous medical devices including tubing, catheters, and pacemaker leads. The elastomer was prepared by mixing one part by weight of curing agent with ten parts by weight of resin, then degassing under vacuum (28–30 in. Hg) for 30 min. The mixture was cured at ~22 °C for 24 h.

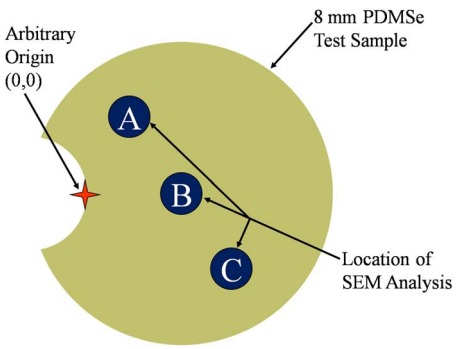

FIG. 2. Locations [(A)–(C)] for scanning electron microscopy (SEM) analysis for 8 mm circular PDMSe samples.

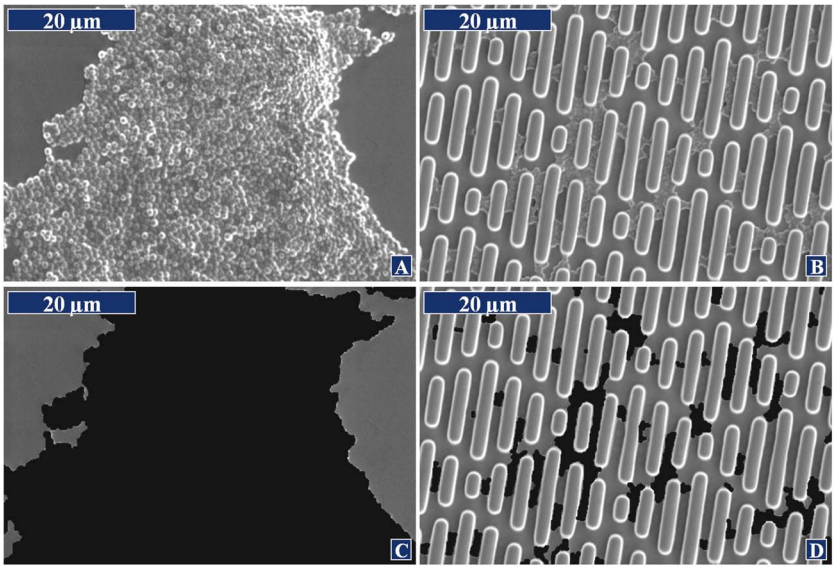

FIG. 3. [(A) and (B)] SEM images (2000×) of *S. aureus* on smooth and topographically modified PDMSe surfaces after 7 day exposure. [(C) and (D)] Processed SEM images of smooth and Sharklet AF™ PDMSe surfaces using MACROMEDIA FIREWORKS®. Bacteria covered areas were outlined and blackened.

B. Sharklet AF™ design and fabrication of topographical molds

The Sharklet AF™ design[24,25] consists of 2 μm wide rectangular ribs of varying lengths ranging from 4 to 16 μm. The ribs of varying lengths are combined into a periodic, diamondlike array at a fixed spacing of 2 μm between neighboring features (Fig. 1). The final, resultant Sharklet AF™ topography in PDMSe was created by replication of silicon wafer molds. Silicon wafer molds were fabricated by first transferring the Sharklet AF™ design to photoresist-coated silicon wafers using photolithographic techniques as previously described.[30] Next, the patterned silicon wafers were deep reactive ion etched to a depth of 3 μm before being cleaned of residual photoresist with an O_2 plasma etch. The etched silicon wafer surfaces were then methylated (via vapor deposition) with hexamethyldisilazane to prevent adhesion. These wafers served as negative molds for topographical replication of the Sharklet AF™ topography at a feature height of 3 μm onto a PDMSe surface.

C. Sample preparation

Silicon molds were replicated into PDMSe to produce ~0.4 mm thick films containing protruding topographical features. Briefly, the PDMSe material components were prepared and mixed as described,[24,25] poured over the silicon wafer molds, and the entire system was pressed between two larger glass plates with the appropriate spacers to produce a 0.4 mm thick film. After curing for 24 h, the PDMSe film was removed from the silicon wafer with protruding topographical features forming the Sharklet AF™ topography on the PDMSe surface (Fig. 1). PDMSe samples of smooth (replicated from an unmodified silicon wafer) and topographically modified were punched out with a circular die 8 mm in diameter. Five replicates each of smooth PDMSe and Sharklet AF™ PDMSe disks were placed into 3 in. Petri dishes (one dish for each day examined) for the growth assay and gas sterilization.

D. *S. aureus* biofilm formation assay

Staphylococcus aureus (ATCC 29213) was subcultured in tryptic soy broth (TSB) growth medium and grown at 37 °C overnight in static conditions. Optical absorbance was measured, serial dilutions were performed, and growth curve and linear optical density-colony-forming unit (CFU) regression were plotted. Bacterial concentration was determined via spectrophotometry by interpolating CFU per milliliter from the linear optical density-CFU regression. Samples were statically immersed in a 10^7 CFU/ml bacterial suspension for up to 21 days. Every day, dishes were put on a rocker for 1 min at 30 rpm and the medium was replaced to allow for continued bacterial growth. Dishes were removed on days 0, 2, 7, 14, and 21. For each removed dish, areas surrounding

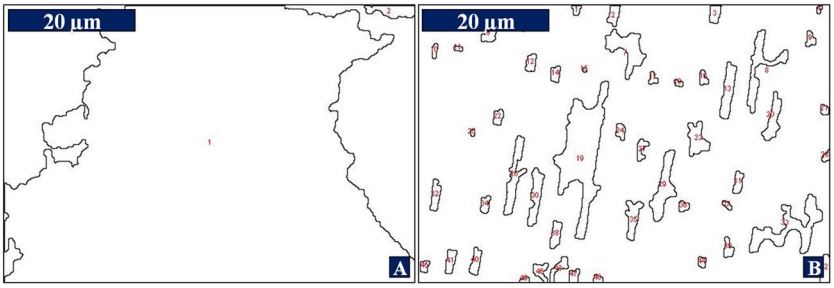

FIG. 4. Grouping and numbering of bacteria colonies as measured by IMAGEJ software. The analysis pictured was conducted on the processed SEM images in Fig. 3. (A) Bacteria coverage on a smooth PDMSe surface was detected as two colonies. (B) Bacteria coverage on a Sharklet AF™ PMDSe surface was detected as over 40 individual colonies of bacteria.

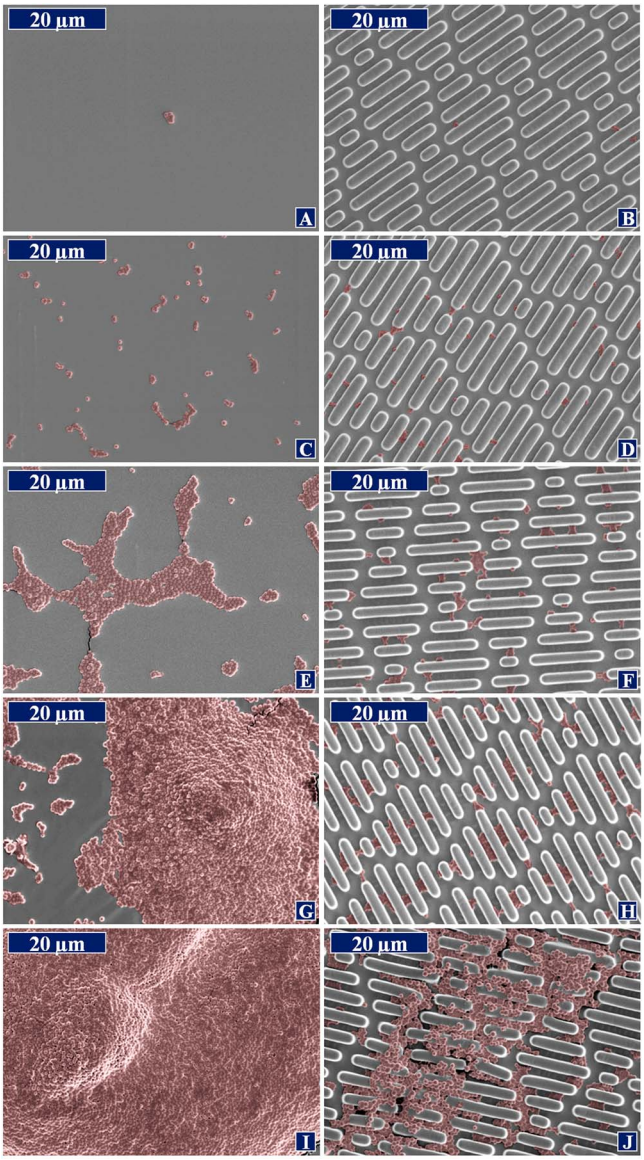

FIG. 5. Representative SEM images of *S. aureus* on PDMSe surfaces over the course of 21 days (areas of bacteria highlighted with color to enhance contrast). On the left are smooth PDMSe surfaces and the right column shows Sharklet AF™ PDMSe surfaces. (A) and (B) day 0, (C) and (D) day 2, (E) and (F) day 7, (G) and (H) day 14, and (I) and (J) day 21.

the samples on the placement grid were rinsed with deionized water using a Pipet-Aid® and aspirated to eliminate nonadherent cells. This rinsing procedure was repeated for a total of three times, and the dish was then put on an orbital rocker for 1 min at 30 rpm. Each sample in the dish was then treated with 20 ml of 10 mM cetyl-pyridinium chloride fixative and allowed to air dry overnight. Another dish exposed only to sterile medium was incubated with the samples for 21 days and served as a negative control.

E. Characterization

Samples were dehydrated in a graded ethanol series of 25%, 50%, 75%, 95%, and 100% at 10 min intervals. Samples were washed twice with hexamethyldisilazane with a 5 min interval between washings, followed by drying using a vacuum desiccator. Each sample was attached to a beveled disk and sputter coated with Au/Pd and imaged with a JEOL 6400 scanning electron microscope (SEM). SEM images at 2000× from areas A, B, and C for each replicate were used to quantify bacterial growth on each surface (Fig. 2).

Biofilms were identified by the presence of microorganisms and exopolymeric matrix. Biofilm growth was estimated by measuring the percent area of coverage of bacteria. To obtain this value, SEM images were first processed using MACROMEDIA FIREWORKS® software to outline and blacken the area containing bacteria and/or biofilm (e.g., Fig. 3).

Processed SEM images were analyzed for percent coverage using IMAGEJ software.[31] Areas of coverage were numbered and outlined, and the total summation of area covered was measured (e.g., Fig. 4). For each replicate, the results for areas A, B, and C are combined to reflect the percentage coverage of bacteria for that specific replicate. Results for each replicate are reported as percent coverage of bacterial colonies.

F. Statistical analysis

The mean value (± standard error) of percent area coverage of bacteria on both smooth and Sharklet AF™ PDMSe surfaces at days 0, 2, 7, 14, and 21 was calculated. Statistical differences were evaluated by a two-way analysis of variance for the factors of "surface" (smooth versus Sharklet AF™) and "day" (0, 2, 7, 14, and 21) followed by Tukey's test for multiple comparisons. Statistical differences were considered at the 95% confidence level.

III. RESULTS

On day 0, individual cells were seen on the surfaces of smooth PDMSe [Fig. 5(A)], while individual cells appeared in the recesses between the protruding features for Sharklet AF™ PDMSe surfaces [Fig. 5(B)]. On day 2, microcolonies of bacteria began to form on the smooth surfaces [Fig. 5(C)], and the Sharklet AF™ surfaces continued to have isolated cells accrete between features [Fig. 5(D)]. Growth of the microcolonies increased on day 7 for the smooth surfaces into early-stage biofilms [Fig. 5(E)]. The Sharklet AF™ surfaces (day 7) continued to exhibit small-sized clusters of bacteria, with no evidence of early-stage biofilm development; the clusters were positioned similar to day 2 in the recesses between protruding topographical features [Fig. 5(F)]. On day 14, the smooth surfaces had the first evidence of mature biofilms [Fig. 5(G)], while the Sharklet AF™ surfaces had a slight increase in the number of small clusters of cells compared to day 7 but still no evidence of early biofilm development or formation [Fig. 5(H)]. On day 21, a significant portion of the smooth PDMSe surfaces was colonized by biofilms [Fig. 5(I)], and biofilms first appeared in isolated areas on the Sharklet AF™ PDMSe surfaces [Fig. 5(J)]. Areas surrounding the large bacterial colonies on the topographical surfaces for day 21 were virtually devoid of adherent bacteria. SEM images of the negative control samples exposed to only TSB media showed no cells.

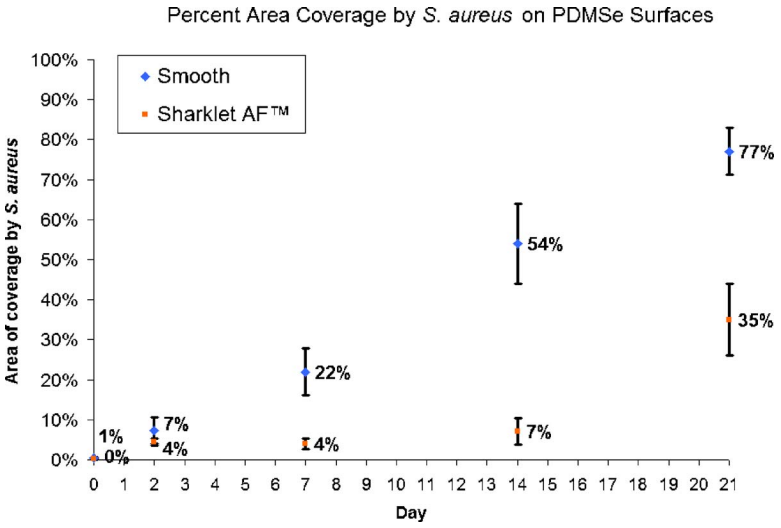

FIG. 6. Mean value of percent area coverage of bacteria on smooth and Sharklet AF™ PDMSe surfaces at various time points. Bars represent±standard error, $n=5$.

Image and statistical analysis indicated that smooth PDMSe samples had significant increases in bacterial coverage for pooled time points (Tukey's test, $p<0.05$), with the first evidence of biofilm on day 7 samples. The Sharklet AF™ samples had significantly lower values of percent area coverage for days 7, 14, and 21 (Tukey's test, $p<0.05$), with biofilm colonies not appearing until day 21. Even on day 21, biofilm colonies covered only isolated areas on Sharklet AF™ samples, with little to no evidence of biofilms or bacterial cells in other areas. The mean value (± standard error) of percent area coverage of bacteria on both smooth and Sharklet AF™ PDMSe surfaces at days 0, 2, 7, 14, and 21 was calculated and is graphically displayed (Fig. 6).

IV. DISCUSSION

Most *in vitro* studies involving *S. aureus* have examined the adhesion behavior over the course of a few hours.[16,19] However, for transcutaneous devices such as catheters, the time frame for biofilm formation is typically 14 days.[7] Thus, the focus of this study was to test the effects of an engineered microtopography on bacterial colonization and biofilm formation for a period of time that extended beyond 14 days. The growth assay parameters included optimized conditions for *S. aureus* colonization and spanned 21 days. To date, this is the first *in vitro* study involving surface topography and *S. aureus* over a time period approximating that of short-term indwelling devices.

Material selection in this study was predicated upon the popularity of silicone as the choice material for molded implants, such as cochlear implants and long-term catheters, despite being shown to have nearly a tenfold greater risk of infection than other polymer materials.[32] The static culture provided for biofilm growth was chosen to represent the most challenging environment for the material surface in the presence of bacteria, as opposed to the low shear dynamics of indwelling catheters. The results of this study strongly suggest that the surface modification of existing silicone devices with the Sharklet AF™ topography may prolong the service life and improve the efficacy of these devices. It is also encouraging to note that the topographical modification of a surface used in this study involves no chemical changes of the biomaterial surface and does not rely on the release of any antibacterial agents.

Both qualitative (e.g., development of extracellular matrix) and quantitative measures of biofilm formation revealed inhibition of biofilm development on PDMSe with Sharklet AF™ microtopography. The results confirm the hypothesis that cells can fit in the recessed regions between the protruded topographical features, but evidence of biofilm formation did not occur on the Sharklet AF™ features until day 21. The raised features could potentially reduce the surface area exposed to bacteria if the channels failed to fill with growth media. However, finding bacteria strictly in the Sharklet AF™ channels speaks against this possibility. Observations of adhered bacteria would suggest that the protruded features of the topographical surface provided a physical obstacle to deter the expansion of small clusters of bacteria present in the recesses into microcolonies. It was at day 21 when bacteria were observed to form small, multilayered colonies within the recesses in order to extend over the protruding features and connect to other isolated colonies. This phenomenon may be the explanation for the delay of early-stage biofilm development to day 21 that was evident on the smooth surface at day 7.

In the context of the "race for the surface" in biomaterials,[3] our engineered surface approach suggests the use of a hierarchy of surface topographies[26] to control bioadhesion. Previous results detailing an engineered topography capable of promoting cell growth[33] can be integrated into the Sharklet AF™ in this study to produce a hierarchical topography for desirable competitive adhesion at the biomaterial surface. One can envision a surface that repels and delays biofilm formation to the extent that host cells, vital to the integration of the biomaterial with the physiological environment, can be established and proliferated on the designed surface.

This study was performed using a highly simplified *in vitro* model. A great deal of work is needed to determine if

observations from this *in vitro* model are borne out *in vivo*. Current research is evaluating the adhesion and biofilm formation tendencies of other biofilm-forming bacteria on Sharklet AF™. Also, the application of the engineered roughness index is being used to predict other engineered topographies that may be effective at inhibiting biofilm formation. Considerations for designing the optimal microtopography for an implantable device will include the interactions with host molecules and impact on fibrous capsule formation.

V. CONCLUSIONS

S. aureus was cultured on PDMSe surfaces for up to 21 days. Biofilms were established after 14 days on the smooth PDMse surfaces whereas an engineered surface microtopography with nonrandom, clearly defined features elicited a negative response. The Sharklet AF™ microtopography disrupted *S. aureus* colonization and biofilm formation without the use of bactericidal agents. Engineered surface microtopographies present a promising means of blocking biofilm development and reducing the rate of biomedical implant infections.

ACKNOWLEDGMENTS

The authors gratefully acknowledge the financial support of the Office of Naval Research, Award No. N00014-02-1-0325 to one of the authors (A.B.B). Special thanks to Sean Royston for his technical assistance in production and fabrication of the engineered topography.

[1]J. W. Costerton, Z. Lewandowski, D. E. Caldwell, D. R. Korber, and H. M. Lappin-Scott, Annu. Rev. Microbiol. **49**, 711 (1995).
[2]J. Costerton, P. Stewart, and E. Greenberg, Science **284**, 1318 (1999).
[3]A. Gristina, Science **237**, 1588 (1987).
[4]J. W. Costerton, G. G. Geesey, and K.-J. Cheng, Sci. Am. **238**(1), 86 (1978).
[5]C. Fux, J. Costerton, P. Stewart, and P. Stoodley, Trends Microbiol. **13**, 34 (2005).
[6]W. Costerton, R. Veeh, M. Shirtliff, M. Pasmore, C. Post, and G. Ehrlich, J. Clin. Invest. **112**, 1466 (2003).
[7]J. W. Costerton, G. Cook, M. Shirtliff, P. Stoodley, and M. Pasmore, in *Biomaterials Science*, edited by Buddy D. Ratner, Allan S. Hoffman, Frederick J. Schoen, and Jack E. Lemons (Elsevier, San Diego, CA, 2004), pp. 345–353.
[8]C. Gordon, N. Hodges, and C. Marriott, J. Antimicrob. Chemother. **22**, 667 (1988).
[9]W. Nichols, M. Evans, M. Slack, and H. Walmsley, J. Gen. Microbiol. **135**, 1291 (1989).
[10]L. G. Harris and R. G. Richards, Injury **37**, S3 (2006).
[11]J. C. Nickel, I. Ruseska, J. B. Wright, and J. W. Costerton, Antimicrob. Agents Chemother. **27**, 619 (1985).
[12]R. M. Donlan and J. W. Costerton, Clin. Microbiol. Rev. **15**, 167 (2002).
[13]R. Schwalbe, J. Stapleton, and P. Gilligan, N. Engl. J. Med. **316**, 927 (1987).
[14]F. Biavasco, E. Giovanetti, M. P. Montanari, R. Lupidi, and P. E. Varaldo, J. Antimicrob. Chemother. **27**, 71 (1991).
[15]K. Hiramatsu, H. Hanaki, T. Ino, K. Yabuta, T. Oguri, and F. C. Tenover, J. Antimicrob. Chemother. **40**, 135 (1997).
[16]P. Vaudaux, P. Francois, B. Berger-Bachi, and D. P. Lew, J. Antimicrob. Chemother. **47**, 163 (2001).
[17]Y. H. An and R. J. Friedman, J. Biomed. Mater. Res. **43**, 338 (1998).
[18]W. Teughels, N. Van Assche, I. Sliepen, and M. Quirynen, Clin. Oral Implants Res. **17**, 68 (2006).
[19]E. Medilanski, K. Kaufmann, L. Y. Wick, O. Wanner, and H. Harms, Biofouling **18**, 193 (2002).
[20]M. Pasmore, P. Todd, S. Smith, D. Baker, J. Silverstein, D. Coons, and C. N. Bowman, J. Membr. Sci. **194**, 15 (2001).
[21]A. Allion, J.-P. Baron, and L. Boulange-Petermann, Biofouling **22**, 269 (2006).
[22]T. Scheuerman, A. Camper, and M. Hamilton, J. Colloid Interface Sci. **208**, 23 (1998).
[23]K. Whitehead, J. Colligon, and J. Verran, Colloids Surf., B **41**, 129 (2005).
[24]M. Carman *et al.*, Biofouling **22**, 11 (2006).
[25]J. F. Schumacher *et al.*, Biofouling **23**, 55 (2007).
[26]J. F. Schumacher, N. Aldred, M. E. Callow, J. A. Finlay, J. A. Callow, A. S. Clare, and A. B. Brennan, Biofouling (to be published).
[27]A. S. Clare and J. A. Nott, J. Mar. Biol. Assoc. U.K. **74**, 967 (1994).
[28]P. Antonelli, J. Lee, and R. Burne, Otol. Neurotol. **25**, 953 (2004).
[29]L. Hoipkemeier-Wilson *et al.*, Biofouling **20**, 53 (2004).
[30]A. W. Feinberg *et al.*, ACS Symp. Ser. **838**, 196 (2003).
[31]W. S. Rasband, IMAGEJ, U.S. National Institutes of Health, Bethesda, MD, http://rsb.info.nih.gov/ij/, 1997–2006.
[32]R. J. Sherertz, in *Infections Associated with Indwelling Medical Devices*, edited by F. A. Waldogel and A. L. Bisno (ASM, Washington, DC, 2000), pp. 111–125.
[33]A. W. Feinberg, W. R. Wilkerson, C. A. Seegert, A. L. Gibson, L. Hoipkemeier-Wilson, and A. B. Brennan, J. Biomed. Mater. Res. (to be published).